International Forum on Aeroelasticity and Structural Dynamics
IFASD 2026
16-19 June 2026, Goettingen, Germany

MULTIDIMENSIONAL LOADS CRITERIA FOR ACTIVE LOAD ALLEVIATION CONTROL DESIGN

Christian Wallace[1] **and Nicolas Fezans**[1]

[1]DLR Institute of Flight Systems
Lilienthalplatz 7, 38108 Braunschweig, Germany
christian.wallace@dlr.de
nicolas.fezans@dlr.de

Keywords: Multidimensional Load Envelope; Load Potatoes; Active Load Alleviation

Abstract: This paper presents a new approach allowing the high-level decomposition of multidimensional load envelope, sometimes referred to as "load potatoes", targets, leading to a set of requirements to complement established control design criteria on the individual load types at each load station. As the key element of the presented method, load case trajectories are mapped onto specific, often skewed, directions of the considered multidimensional space, enabling converting multidimensional load envelope targets into series of elementary one-dimensional optimisation requirements. The stated method addresses the opportunity to formulate optimisation criteria which enable the flight control designer to express target deformations of multidimensional load envelopes. Combined with a tightening/relaxation of the weights and constraints, the method allows shaping these multidimensional load envelopes, provided that sufficient control authority is available. Whilst the control design method is applicable to all types of load alleviation controllers or any similar multi-dimensional problems, its principle is explained and illustrated with the example of the design of a gust load alleviation controller.

1 INTRODUCTION

The certification process for a new aircraft type requires the consideration of different load cases (manoeuvre cases, gust cases, etc.) to determine critical structural loads. The airframe must be proven to withstand these loads, meaning that the structural loads associated with the load cases have a significant influence on the design of the primary structure. A successful reduction of critical loads leads to potential weight savings, which would be in line with the common objective of significantly reducing the emissions of modern transport aircraft.

Active control technologies [1–4] provide the opportunity to alleviate structural loads, to resize the aircraft's primary structure, and consequently save weight [5–7]. For both passive and actively controlled structures, the structural optimisation in terms of effective mass reduction depends on affecting cut loads in several load dimensions. [8] presents an example of a design study considering and comparing various load alleviation systems with the passive (open-loop) case and between each other. The precise simultaneous analysis of different cut loads (e.g. bending and torsion) is therefore necessary, which is already used regularly today. Load alleviation control functions are often tuned with criteria which consider combinations of load stations and directions, however considering each of them individually (e.g. [9–12]). The consideration of multiple structural load dimensions and the inclusion of numerous load cases go along with a complex load structure, leading to a superposition of several convex hulls ("load potatoes") at each structural point (load station). Depending on the control function considered, some of these convex hulls can be affected and others cannot. A typical target in the case of a gust load alleviation (GLA) control design problem would be to reduce the gust load envelopes to the union of the load envelopes from other load types (as a target envelope, e.g. a composition of manoeuvre loads, landing loads, etc.). In other words, the ultimate goal would be that no gust load case dominates the other loads and is partly responsible for the sizing of the structure. Depending on the available sensors, actuators, and the design of the aircraft, this goal may not be fully achievable.

Regardless of whether this goal can be achieved, the underpinning assumption behind the present work is that the designer may use active control means to reshape the gust load envelope and, by doing so, be able to reduce the weight of the aircraft. This work does not attempt to define the combinations of multidimensional load targets and stations that allow optimising the weight of the aircraft. Instead, it focuses on the definition of a (linear) robust control design approach which allows the synthesis of controllers based on such multidimensional envelopes. Whilst analysing a set of time-series to estimate the gust load envelope and comparing this envelope to the target envelope is straightforward, defining transfer functions and the corresponding weightings/templates to drive a frequency-domain control synthesis algorithm towards the target objective is less obvious.

This paper is structured as follows. Section 2 presents the underlying multidimensional optimisation problem, followed by the mathematical parametrisation of the multidimensional load space in Section 3. Section 4 then derives a method to choose adequate (one-dimensional) directions and describes the introduction of H_2 control specifications based on *Discrete Gust Impulse Filters* to be used in the control design workflow which is discussed briefly in Section 5. Lastly, Section 6 provides conclusions and an outlook to future work.

2 MULTIDIMENSIONAL OPTIMISATION PROBLEM

A schematic representation of the main objective is provided in Figure 1. On the left part, the gust loads envelope (here shown for two cut load dimensions, namely the bending moment M_x and torsional moment M_y) is overlaid in blue on top of some target load envelope in orange. A typical target in the case of a gust load alleviation (GLA) control design problem would be to reduce the gust load envelopes to the union of the load envelopes from other load types (as a target envelope, e.g. a composition of manoeuvre loads, landing loads, etc.).

For the imaginary case shown in Figure 1, the blue region (gust load envelope) is dominating the load envelope on the left plot for positive values of the bending moment. By *squeezing* the gust envelope (in blue) to fit within the target envelope (orange), the peak loads along certain directions of this multidimensional space (here illustrated with two dimensions) are reduced and, at the same time, increases along other directions are tolerated.

The gust load cases for the certification of large aeroplanes are defined in CS 25.341a [13]. Gusts with certain scales (9 to 107 m) and amplitudes need to be considered in all directions. To ensure a detailed evaluation of the aircraft behaviour, a representative set of gust load cases must be selected for analysis. This includes the evaluations for different mass configurations and flight points. In practice, these requirements result in the evaluation of hundreds to thousands of load cases and the gust load envelope is usually defined as the convex hull of all these load cases.

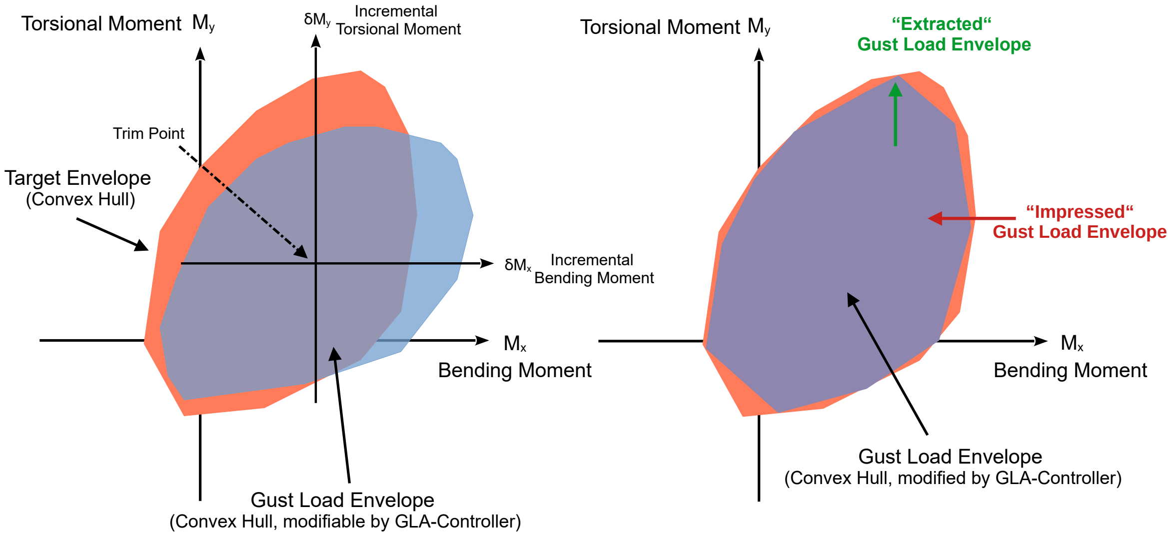

Figure 1: Merging a gust load envelope with a target envelope via morphing multidimensional loads. The left-hand side shows the status without a gust load alleviation controller function, the right-hand side shows an ideal state with a gust load alleviation controller function in operation.

The development of controller functions typically uses linear aircraft models, usually in state-space form. Often the behaviour of the aircraft is (nearly) linear and whilst nonlinear effects can occur (e.g. with transonic shocks, buckling, or even nonlinear elements), considering such effects in the initial controller design does not seem to be a standard practice. The linear control theory provides very powerful tools which largely simplifies the controller design, fine tuning, and evaluation.

For the design of GLA control functions, aeroelastic models with a set of structural cut loads as output variables are usually used. A fundamental characteristic of linear systems is that their equilibrium is always at zero. In the case of such linear aeroelastic models, this means that they describe the dynamics of a delta-state and delta-outputs, i.e. with respect to the operating point around which they were linearised. While this aspect is well-known, this basic fact should be kept in mind as the target loads envelopes are defined as absolute load values. For each flight point and mass case, the *origin* or *zero-state* corresponds to a slightly different absolute position and therefore relative position with respect to the target load envelope. So, the incremental load envelopes (converted from the fixed target load envelope) depend on each flight point and mass case.

An exemplary gust load envelope, simulated with the Generic Long-Range Aircraft model [11, 12, 14], can be seen in Figure 2, enclosing incremental gust load trajectories. In the example shown, the chosen set of gust load cases consists of symmetrical gusts with eight different gust lengths. The gust lengths are distributed equidistantly between 9 m and 107 m. All gust lengths are simulated separately as an upward and a downward gust. The trajectories are coloured in grey. Two gust load cases (same gust length, but simulated as an upward gust and a downward gust) are highlighted in colour for clarity. The simulated trajectories are embedded in a two-dimensional M_x-M_y-cut load plane (two-dimensional cut load space), spanned by the bending moment M_x-direction (abscissa) and the torsional moment M_y-direction (ordinate). The responses to the two opposite gusts are opposite to each other for every variable and point-symmetrical with respect to the zero-state in the multidimensional space considered.

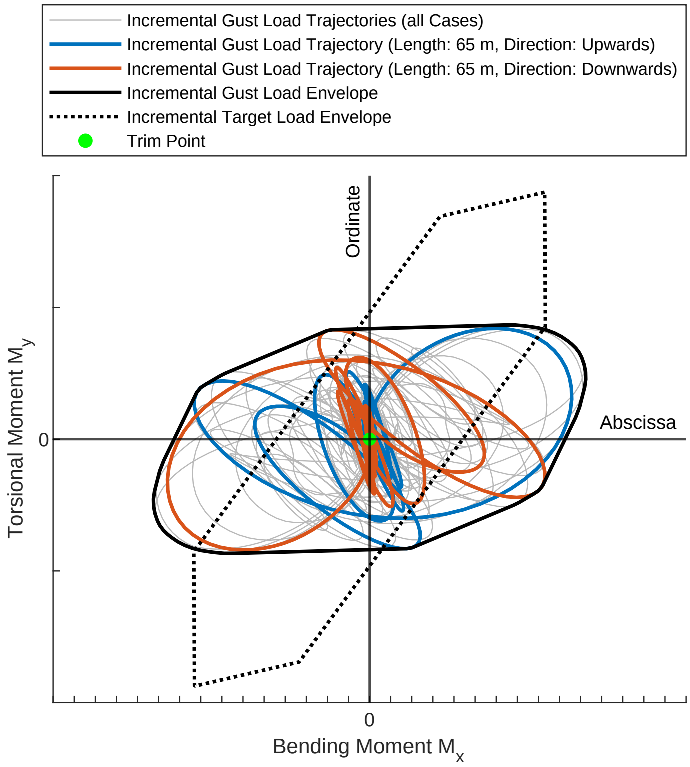

Figure 2: Exemplary gust load envelope including corresponding gust load trajectories and optimization targets. The axes (for the cut load moments) uses unequal scaling for visualisation purposes.

The point-symmetrical responses of linear systems when excited with inputs of opposite signs means that the incremental loads envelope specifications are necessarily point-symmetrical in practice. If different limits are set for two opposite directions, the only relevant specification is the one that is the closest to the origin (trim condition). The other one is never violated without also violating the first.

In the following, all target envelopes used are exemplary convex hulls, defined for the sole purpose of explaining the proposed method. Their shapes and orientations are most likely far from any meaningful target envelopes with the usual reference frame definitions for the wings. The relative spatial position of both envelopes to each other defines spatial areas of the gust load envelope that should be "pushed towards zero" or could "move away from zero". In the (very artificial) example of Figure 2, the multidimensional target loads are exceeded, especially in terms of bending moment (abscissa). The control design algorithm would have to try squeezing the gust loads more or less horizontally. A rotation of the whole envelope by about $45°$ would also reduce the discrepancy between the incremental gust load envelope and the target load envelope.

When considering the individual loads, e.g. bending moment or torsional moment, only the deviation along that corresponding axis is considered. In other words, the multidimensional loads are projected on the corresponding axes. Figure 3 shows the same two time responses of the bending and torsional moments for the cases highlighted in blue and red in Figure 2. The point-symmetry around the trim point between an upward gust load case and the corresponding downward gust load case is also evident in the time responses as each of the two responses is the opposite of the other.

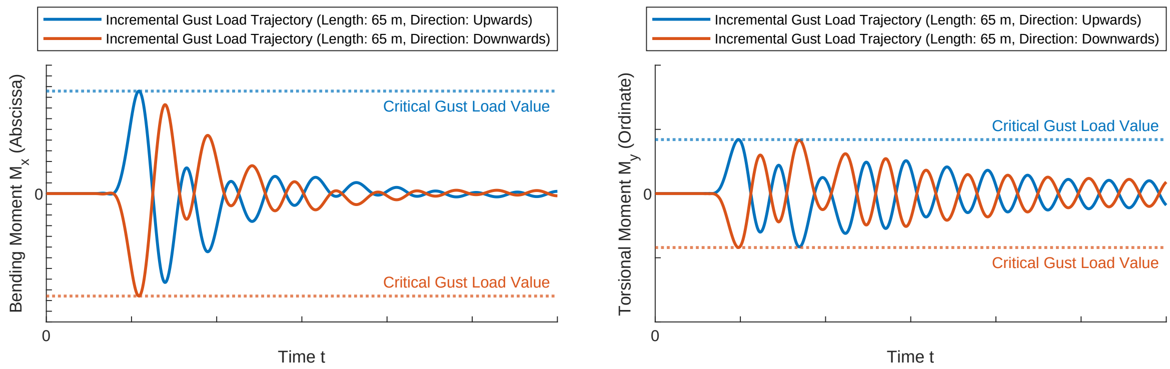

Figure 3: Time responses for the bending and torsional moment for the cases highlighted in Figure 2.

3 PARAMETRISATION OF THE MULTIDIMENSIONAL LOAD SPACE

This section presents a series of symbol definitions and transformations used to describe specific directions in the considered multidimensional space. For simplicity, the parametrisation is mostly illustrated for a two-dimensional space, and only tests with two dimensions were conducted so far, but the ideas presented in this work should also be applicable to more dimensions.

3.1 Definition of Directions in the Considered Multidimensional Space

Most engineers and scientists needing to describe a direction in a two-dimensional space will probably start with defining a reference direction and then can describe any other direction with an angle with respect to this reference direction. Figure 4 shows such a definition, for instance taking x_1 as reference direction and the angle φ_0 as reference angle. Such a definition works well in the two-dimensional case, but angle-based parametrisations will become rapidly cumbersome in higher dimensions.

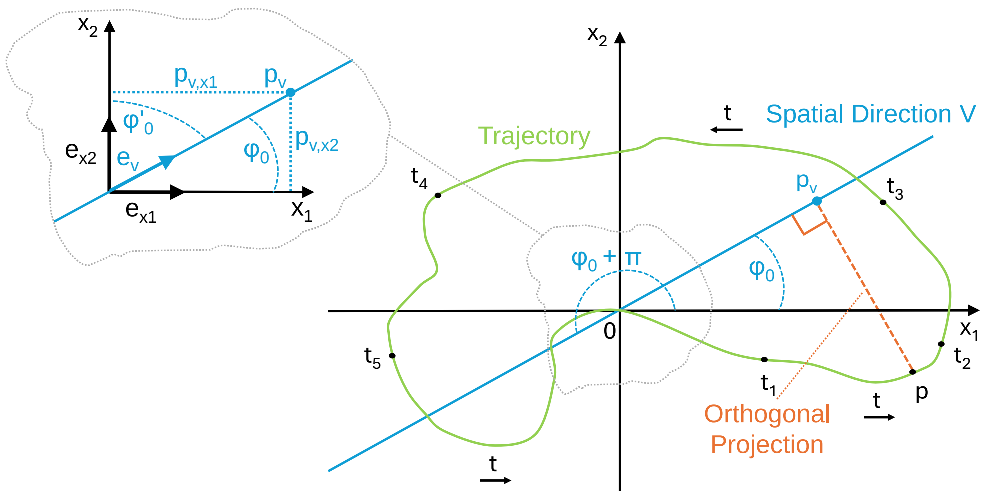

Figure 4: Schematic representation of a two-dimensional plane subdivided by an additional one-dimensional spatial direction (line through the origin)

In higher dimensions a vector (series of components) appears preferable. In the example shown in Figure 4, the unit vector e_v in the direction V can simply be described by the vector

$$\mathbf{e}_v = \begin{bmatrix} e_{v,x1} \\ e_{v,x2} \end{bmatrix} = \begin{bmatrix} \cos(\varphi_0) \\ \sin(\varphi_0) \end{bmatrix} \tag{1}$$

and in n dimensions, a $n \times 1$ vector will be sufficient to describe the direction.

3.2 Orthogonal Projection

When considering the direction V (in blue in Figure 4), each point $\mathbf{p}$ of the trajectory is projected onto the direction V as follows:

$$\mathbf{p}_v = \langle \mathbf{p}, \mathbf{e}_v \rangle \, \mathbf{e}_v \;, \tag{2}$$

with $\langle \mathbf{a}, \mathbf{b} \rangle$ being defined as the scalar product between vectors $\mathbf{a}$ and $\mathbf{b}$ and $\mathbf{e}_v$ being the unit vector in the direction V as defined in eq. (1). The corresponding linear coordinate along direction V is therefore simply $\langle \mathbf{p}, \mathbf{e}_v \rangle$.

3.3 Normalisation Based on Distance to the Target Envelope

In order to be able to evaluate the spatial position of a projected trajectory to the target envelope, a normalisation is introduced. This is explained below using the example of the two-dimensional M_x-M_y-cut load space.

Within the M_x-M_y-plane the incremental bending moment time response $\delta M_x\,(t)$ corresponds to a deviation along the abscissa, and the incremental torsional moment time response $\delta M_y\,(t)$ corresponds to a deviation along the ordinate. The occurring peak magnitudes

$$\delta \hat{M}_{()} = \max_t |\delta M_{()}(t)| \tag{3}$$

of each incremental system response can be used to formulate relative optimisation requirements. Additionally, the intersection points between a chosen spatial direction and specific[1] "facets" (here edges) of the incremental target envelope define (identical, but sign-inverted) incremental reference values (T_+ and T_-) for optimisation purposes. Hence, an incremental load ratio according to

$$\kappa = \frac{\delta \hat{M}_{()}}{|T_+|} = \frac{\delta \hat{M}_{()}}{|T_-|} \tag{4}$$

can be defined. This ratio indicates a spatial direction-dependent potential, which is reflected either in the need to alleviate gust loads ($\kappa > 1$), or an allowable increase in gust loads ($\kappa < 1$) or no need to affect critical gust load values ($\kappa = 1$).

[1] The selection of the "facets" results from the choice of direction, which is explained in the following chapter.

4 DEFINING THE ONE-DIMENSIONAL OPTIMISATION REQUIREMENTS

4.1 Choosing the Adequate One-Dimensional Directions

Within the multidimensional space considered, a set of directions on which the multidimensional loads are considered needs to be defined. As it will be shown in the following, only very specific directions must be considered to obtain the desired control design objectives/constraints.

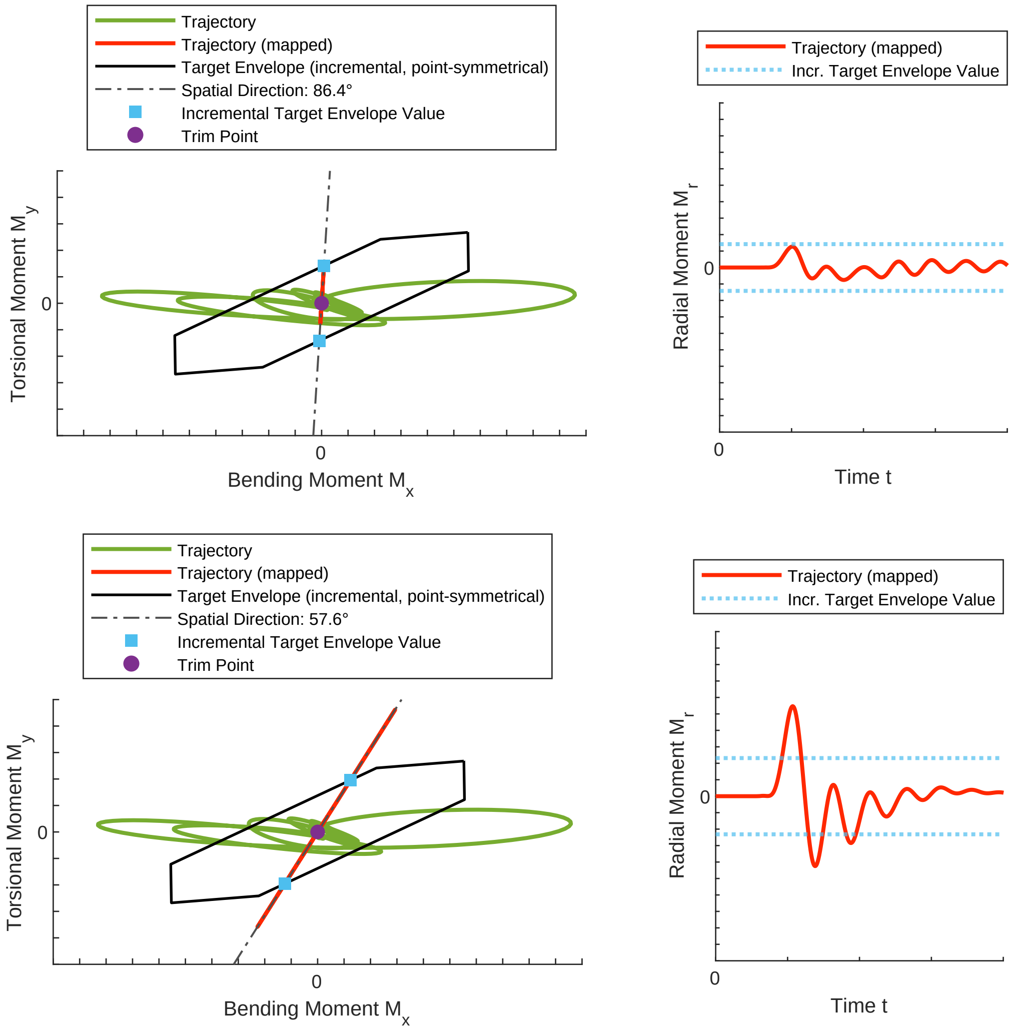

Figure 5: Left: trajectories of an upward gust load case (gust length H = 65 m), mapped onto different spatial directions. Right: resulting mapped trajectories are in the time domain.

To illustrate why certain directions are unsuited, a case is constructed based on an upward gust with a length of 65 m (only one case) and some imaginary two-dimensional specifications. First, fairly random directions ($\varphi_{0,1} = 86.4°$ and $\varphi_{0,2} = 57.6°$) are considered in Figure 5. In this figure, the two-dimensional loads are shown in the left column in green and the target envelope as black polygons. Both remain identical in all cases. The considered directions are represented as a grey dash-dotted line and the projection of the multidimensional loads (green line) onto the considered direction is represented in red both in the multidimensional diagram on the left and on the one-dimensional (projected) time series on the right. For the direction $86.4°$ (top row), the result may seem reasonable, but the other results raise some questions. In particular, a significant violation of the incremental target envelope values is determined for the case with a direction of $57.6°$ (lower row, right plot). However, looking at the corresponding multidimensional plot on the left side, it is obvious that the green line remained within the two threshold values for the considered direction (blue squares). Indeed, the projection of the green line onto the $57.6°$ direction exceeds the threshold values.

These directions are obviously not adequate for the intended purpose. The problem is actually even worse than shown on these examples. For example, a trajectory point located just inside the envelope near the top right corner of the target envelope would be projected outside of the segment between the target threshold values (blue squares) for $\varphi_{0,1} = 86.4°$.

Using the properties of the symmetrised target envelopes and especially the fact that the considered domains are convex, it can be concluded that only the directions that are perpendicular to the target load envelope boundary will never project a point that is located within the target envelope outside of the acceptable segment. This is illustrated in Figure 6. In this figure, the three directions that are perpendicular to the target envelope "facets" are being used.

Indeed by selecting a direction perpendicular to the envelope, the projection onto this direction ends up being parallel to the local tangent of the envelope border, which is a sufficient condition for *not leaving the interior* of the convex set through this projection. What may happen though is the projection of a point that is outside the envelope onto the segment between the two threshold values (so *entering* the set via this projection). This case can be seen in the middle row in Figure 6 (case with $94.39°$). In this case, points from the green line that were outside of the set were projected into the set. This behaviour is not a problem, because it can easily be demonstrated that there will always be another direction considered at the same time and for which this will not happen.

So to sum up, when considering all and only the directions that are perpendicular to at least a piece of the contour of the target envelope border, the following properties are guaranteed:

- For every point within the target envelope, every projection operation will always yield a one-dimensional criterion that will not be exceeded for this point ($\max(\kappa_i) \leq 1$).
- For every point outside the target envelope, there is at least one of the considered direction leading to a one-dimensional criterion that this point will violate ($\max(\kappa_i) > 1$).

This result also means that instead of discretising all possible directions in a multidimensional space, the number of directions to consider is half the number of facets of the target envelope. Due to the point symmetry, every facet has a symmetrical one, but they share the same perpendicular direction. So even in dimension 3, 4, 5, etc. as long as the number of facets describing the target envelope remains reasonable, so will the number of direction to consider. This also means that the worst possible case would be to consider a target load envelope defined as a continuous curve as this would potentially yield an infinite number of directions to consider. In practice, a discretisation of the shape using a reasonable number of facets will probably always be possible.

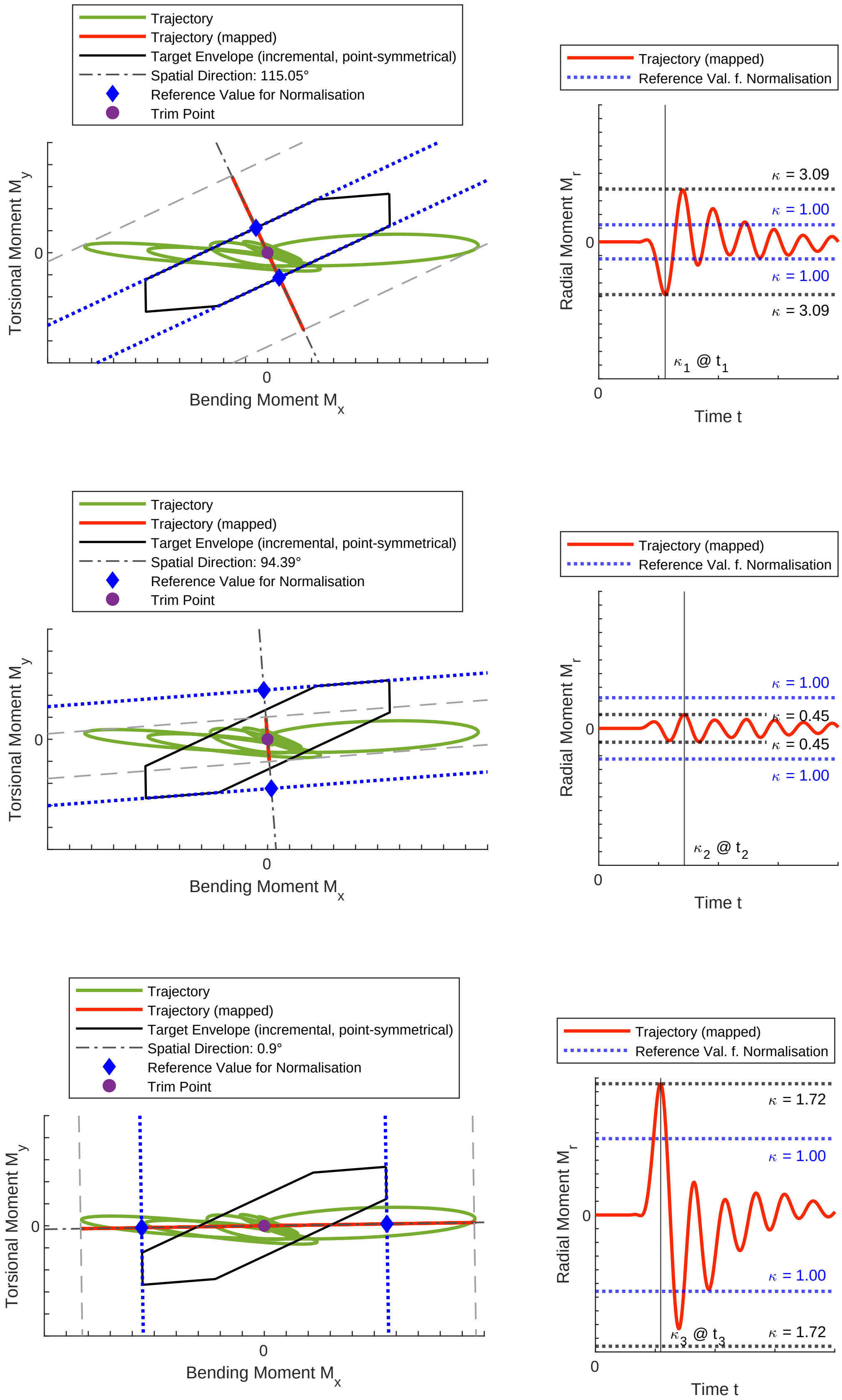

Figure 6: Left: trajectories of an upward gust load case (gust length H = 65 m), mapped onto perpendicular spatial directions. Right: resulting mapped trajectories are in the time domain

4.2 Frequency-Domain Specifications via Discrete Gust Impulse Filters

With the proper parametrisation and the right set of directions being defined, one main question remains: how should a suitable control design requirement be defined for the considered directions?

In [15, 16] an H_2 specification using so-called *Discrete Gust Impulse Filters* (DGIF) was introduced, after the authors regularly noticed that a reduction of the H_∞ norm of the transfer from gust/wind input(s) to the load stations quite often yield an increase of the peak loads on one-minus-cosine gust encounter simulations. This is because reducing the peak gain sometimes had the effect of increasing the average gain (i.e. over a wide range of frequencies).

For a given gust length, a low-order filter can be created as an approximation of a finite impulse response (FIR) filter. The authors of [16] have also provided the low-order filter coefficients as well as the analytical equations for adapting them to different gust lengths. It was also shown experimentally that the DGIF-weighted H_2 specification better correlates with the time-domain peak response to the corresponding gust length than an unweighted H_2 specification, an unweighted H_∞ specification, and a DGIF-weighted H_∞ specification [16, Fig. 11].

One drawback of the DGIF-weighted H_2 specifications is that a different weighting function is needed for each gust length, which leads to a multiplication of the objectives in the tuning. With proper auto-tuning strategies the same authors could handle the addition and iterative weight adaption needed to manage numerous transfer functions and DGIF-weighted specifications [17]. This auto-tuning process is currently being extended to handle the multidimensional criteria proposed in this work with DGIF H_2 specifications applied to the selected directions in the multidimensional load space.

5 SUMMARY OF THE CONTROL DESIGN WORKFLOW

To be able to put the previous ideas into practice, it is essential to integrate the novel criteria into an iterative optimisation process, executing a robust tuning of free controller parameters in the frequency domain. This workflow is roughly illustrated in Figure 7. The left-hand area (highlighted in pink) comprises the requirement management, in which the new multidimensional criteria are applied.

The designer (highlighted in red) controls the process and decides which data and models from the databases and which controller structures are to be used. The selection and processing of the structural load data determines how the target envelopes for the controller optimisation will be composed. It is possible to consider different realistic load subsets (e.g. manoeuvre loads, gust loads, etc., often results of high-fidelity simulations) in the process, and at the same time, it is also possible to define artificial load targets (as used in the current work).

The absolute target envelopes are then converted into incremental values for each individual aircraft model. This results in different target envelopes, which are convex but each have a (potentially) different shape. The individual set of "facets" of the incremental target envelopes determine the set of critical spatial directions to be selected, which is then used to define the controller requirements automatically.

The entire optimisation problem, consisting of several aircraft models, each with individual sets of optimisation criteria, is automatically assembled. The latter includes the extension of the models by the DGIF. The optimisation algorithm evaluates the loads of the aircraft models in each iteration step. The analysis is performed automatically for all combinations of flight points and mass cases, as well as any load stations and load dimensions. The aircraft models themselves are available in several versions. There are at least two variants provided, one for evaluation purposes and one model specifically for tuning of the controller parameters. The latter are reduced in the number of states compared to the models for the time simulations, which guarantees fast performance within the controller optimisation.

The final evaluation of the (load alleviation) performance of the controller is executed in a simulation environment that takes i.a. non-linear effects into account. This includes saturations of the actuators as well as realistic sensor dynamics [14].

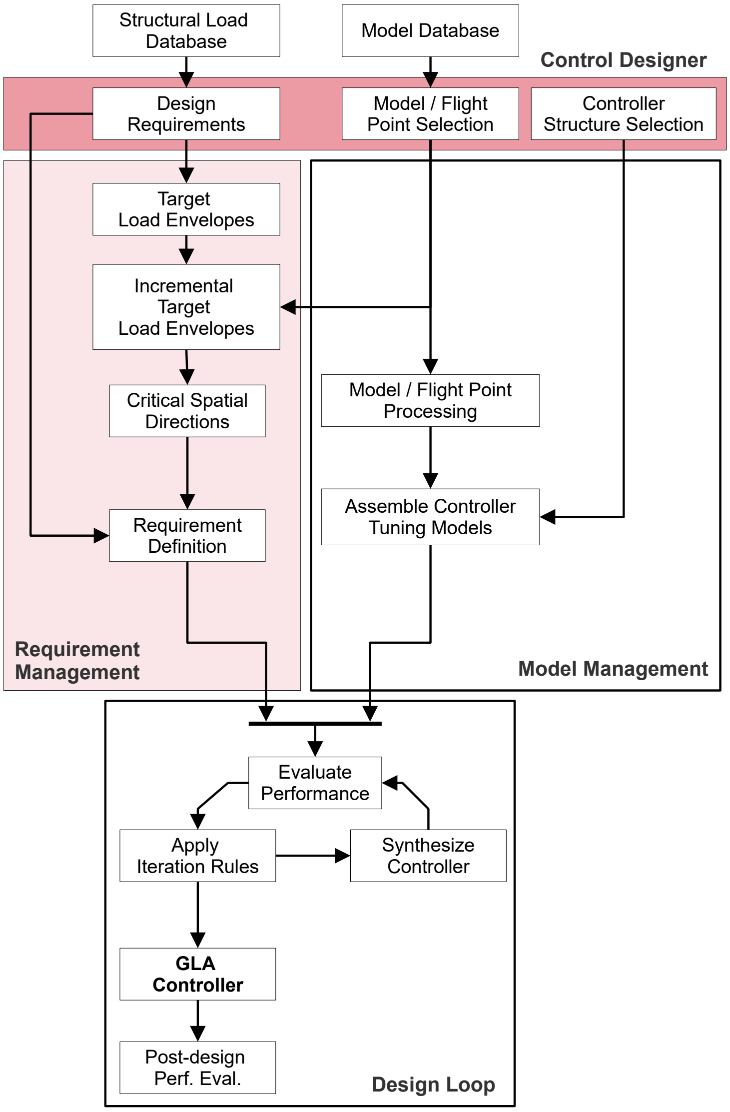

Figure 7: Control design workflow used by the multidimensional loads criteria

6 CONCLUSIONS AND OUTLOOK

This paper introduced a novel type of control specifications giving control designers the possibility to shape multidimensional load envelopes. They use criteria based on the recently introduced discrete gust impulse filters, but, instead of use them one one-dimensional loads, they are applied to arbitrary linear combinations of load outputs of the aeroelastic aircraft. This allows the evaluation and penalisation of system responses to these combined load outputs. Choosing adequate combination of loads, i.e. directions within the multidimensional load space, allows "pushing" specific areas toward the target load envelope. In other areas, load increases may be tolerated.

The ability to shape gust load envelopes via these new criteria opens up the possibility to fine tune the loads envelope to match the needs of the structural sizing team/specialists (required input for the control designer). This new concept is currently being investigated and integrated within a (semi-)auto-tune process, whose sketch was presented as well. On the long-term coupling this kind of capabilities with powerful structural sizing tools seems possible and attractive. The combination of load types and dimensions which make sense to consider for different parts of the airframe remains unclear at this stage and should be investigated.

7 REFERENCES

[1] Livne, E. (2018). Aircraft active flutter suppression: State of the art and technology maturation needs. *Journal of Aircraft*, 55(1), 410–450, doi: 10.2514/1.C034442.

[2] Alam, M., Hromcik, M., and Hanis, T. (2015). Active gust load alleviation system for flexible aircraft: Mixed feedforward/feedback approach. *Aerospace Science and Technology*, 41, 122–133, doi: 10.1016/j.ast.2014.12.020.

[3] Fournier, H., Massioni, P., Tu Pham, M., et al. (2022). Robust Gust Load Alleviation of Flexible Aircraft Equipped with Lidar. *Journal of Guidance, Control, and Dynamics*, 45(1), 58–72, doi: 10.2514/1.G006084.

[4] Wuestenhagen, M. (2023). Gust load alleviation control of aircraft with varying mass distribution. In *AIAA SciTech 2023*. pp. 1–17, National Harbor, USA: AIAA, doi: 10.2514/6.2023-0371.

[5] Wykes, J. H. (1968). Structural dynamic stability augmentation and gust alleviation of flexible aircraft. In *AlAA 5th Annual Meeting and Technical Display*. pp. 1–21, Philadelphia, PA, USA: AIAA, doi: 10.2514/6.1968-1067.

[6] Sensburg, O., Becker, J., Lusebrink, H., et al. (1982). Gust load alleviation on Airbus A300. In *ICAS 1982*. Seattle, Washington, USA: ICAS, `https://www.icas.org/icas_archive/ICAS1982/ICAS-82-2.1.1.pdf`. ICAS-82-2.1.1.

[7] Payne, B. (1986). Designing a load alleviation system for a modern civil aircraft. In *ICAS 1986*. London, UK: ICAS, `https://icas.org/icas_archive/ICAS1986/ICAS-86-5.2.3.pdf`. ICAS-86-5.5.3.

[8] Handojo, V., Himisch, J., Bramsiepe, K., et al. (2022). Potential estimation of load alleviation and future technologies in reducing aircraft structural mass. *Aerospace*, 9(8). ISSN 2226-4310, doi: 10.3390/aerospace9080412.

[9] Cavaliere, D., Fezans, N., Kiehn, D., et al. (2022). Gust load control design challenge including lidar wind measurements and based on the common research model. In *AIAA SciTech 2022 Forum.* , San Diego, CA, USA: AIAA, doi: 10.2514/6.2022-1934.

[10] Fezans, N., Wallace, C., Kiehn, D., et al. (2022). Lidar-based gust load alleviation - results obtained on the Clean Sky 2 Load Alleviation Benchmark. In *IFASD 2022*. pp. 1–29, Madrid, Spain: IFASD, doi: 10.60801/IFASD-2022-155.

[11] Wallace, C. and Fezans, N. (2023). Lidar-based gust load alleviation - results obtained on a Generic Long Range Aircraft configuration. In *Aerospace Europe Conference 2023.* , Lausanne, Switzerland: EUCASS / CEAS, doi: 10.13009/EUCASS2023-564.

[12] Wallace, C. and Fezans, N. (2024). Lidar-based gust load alleviation - increasing the load reduction potential through a two-degree-of-freedom controller architecture. In *IFASD 2024*. The Hague, The Netherlands: IFASD, pp. 1–25. IFASD-2024-163.

[13] European Union Aviation Safety Agency (EASA) (2021). Certification specifications and acceptable means of compliance for large aeroplanes (CS-25) - Amendment 27. `https://www.easa.europa.eu/en/document-library/certification-specifications/cs-25-amendment-27` (2021).

[14] Wallace, C., Schulz, S., Fezans, N., et al. (2022). Evaluation environment for cascaded and partly decentralized multi-rate load alleviation controllers. In *ICAS 2022*. Stockholm, Sweden: ICAS, pp. 1–15, `https://www.icas.org/ICAS_ARCHIVE/ICAS2022/data/preview/ICAS2022_0656.htm`.

[15] Cavaliere, D. and Fezans, N. (2022). Recasting discrete 1-cosine gust requirements as frequency domain specifications for load alleviation control design. In *IFASD 2022.* , Madrid, Spain: CEAS, doi: 10.60801/IFASD-2022-143. IFASD-2022-143.

[16] Cavaliere, D. and Fezans, N. (2024). Toward Automated Gust Load Alleviation Control Design via Discrete Gust Impulse Filters. *Journal of Guidance, Control, and Dynamics*, 1–14. ISSN 0731-5090, 1533-3884, doi: 10.2514/1.G007762.

[17] Cavaliere, D. and Fezans, N. (2024). A practical approach to automated multiobjective gust load alleviation control design in a structured H_2/H_∞ framework. In *Proceedings of the 2024 CEAS EuroGNC conference*. pp. 1–26, Bristol, UK: CEAS, doi: 10.82124/CEAS-GNC-2024-042.

COPYRIGHT STATEMENT